

Many-body effects in x-ray absorption and magnetic circular dichroism spectra within the LSDA+DMFT framework

O. Šipr,^{1,*} J. Minár,² A. Scherz,³ H. Wende,⁴ and H. Ebert^{2,†}

¹*Institute of Physics of the ASCR v. v. i., Cukrovarnická 10, CZ-162 53 Prague, Czech Republic*

²*Universität München, Department Chemie und Biochemie,
Butenandtstr. 5-13, D-81377 München, Germany*

³*Stanford Institute for Material and Energy Science,
SLAC National Accelerator Laboratory, Menlo Park, California, USA*

⁴*Universität Duisburg-Essen, Fakultät für Physik and Center for Nanointegration
Duisburg-Essen (CeNIDE), Lotharstr. 1, 47048 Duisburg, Germany*

(Dated: December 19, 2018)

The theoretical description of photoemission spectra of transition metals was greatly improved recently by accounting for the correlations between the d electrons within the local spin density approximation (LSDA) plus dynamical mean field theory (DMFT). We assess the improvement of the LSDA+DMFT over the plain LSDA in x-ray absorption spectroscopy, which — unlike the photoemission spectroscopy — is probing unoccupied electronic states. By investigating the $L_{2,3}$ edge x-ray absorption near-edge structure (XANES) and x-ray magnetic circular dichroism (XMCD) of Fe, Co, and Ni, we find that the LSDA+DMFT improves the LSDA results, in particular concerning the asymmetry of the L_3 white line. Differences with respect to the experiment, nevertheless, remain — particularly concerning the ratio of the intensities of the L_3 and L_2 peaks. The changes in the XMCD peak intensities invoked by the use of the LSDA+DMFT are a consequence of the improved description of the orbital polarization and are consistent with the XMCD sum rules. Accounting for the core hole within the final state approximation does not generally improve the results. This indicates that to get more accurate $L_{2,3}$ edge XANES and XMCD spectra, one has to treat the core hole beyond the final state approximation.

PACS numbers: 78.70.Dm,75.10.Lp,71.15.Mb
Keywords: correlations,DMFT,XANES,XMCD

I. INTRODUCTION

X-ray absorption spectroscopy (XAS) evolved into a powerful technique for studying electronic as well as geometric structure of solids. Its main strength include chemical selectivity, angular-momentum selectivity and ability to provide detectable signals even for low amounts of material. This makes it well-suited for studying defects, adsorbates, or nanostructures. For studying magnetism, x-ray magnetic circular dichroism (XMCD) spectroscopy, based on exploring the energy-dependence of the difference in the absorption of left- and right-circularly polarized x-rays in a magnetized sample, proved to be a very powerful tool.¹

An efficient use of x-ray absorption spectroscopy requires a significant input from theory. *Ab initio* calculations of x-ray absorption near-edge structure (XANES) and XMCD are usually quite successful in reproducing the positions of spectral peaks, fairly successful in reproducing their intensities and less successful in reproducing detailed shapes of the peaks. The severity of the failures of the theory varies depending on what material is studied, which absorption edges are involved and what purpose the spectroscopic measurement serves.

Magnetic $3d$ elements are often used in artificial structures to form materials with properties that are interesting both fundamentally and for their possible technological application. XAS at the $L_{2,3}$ edges of Fe, Co, and Ni

is used to get information about electronic states of the d character, which dominate close to the Fermi energy E_F . *Ab initio* calculations based on the local spin density approximation (LSDA) to density functional theory suffer here from some common deficiencies. One such deficiency is the inability to reproduce correctly the ratio of the intensities of the L_3 and L_2 white lines in the XANES. This has been ascribed to the lack of proper dynamic treatment of the core hole.^{2,3} Other common deficiencies of *ab-initio* calculations include lack of asymmetry of the theoretical XANES white line and underestimated the ratio of the L_3 and L_2 XMCD peak intensities.^{1,4,5} Having an *ab-initio* method able to deliver a more accurate quantitative agreement with experiment would be a great help when dealing with complex systems. The procedurally simple XMCD sum rules^{6,7} proved to be very powerful in interpreting experiments but their use has limitations. A more robust way is to compare measured spectra to spectra of a well-defined reference material. The properties of the reference material may, nevertheless, differ from the properties of the investigated system and, moreover, a suitable reference may not be available. In such situations, a comparison with accurate and reliable calculations may be very useful.⁸⁻¹⁰

Even though the $3d$ transition metal (TM) elements can be seen as moderately correlated materials, there are known effects where including correlations is necessary. E.g., the orbital magnetic moment μ_{orb} is underestimated by the LSDA and improved results can be obtained by

accounting for the enhancement of the orbital polarization either via the scheme of Brooks (OP Brooks)¹¹ or via the LSDA+ U scheme.^{12,13} These schemes, however, account only for static effects of the electron self-energy. To describe the spectra, dynamical effects should be included as well. This can be achieved via the LSDA plus dynamical mean field theory (DMFT) scheme. The LSDA+DMFT formalism proved to be rather successful when dealing with the photoemission spectra of $3d$ transition metals (TMs).^{14–17} One can, therefore, expect that this formalism might lead to a substantial improvement also for XANES and XMCD spectra. In particular, as the LSDA+DMFT method provides correct values for μ_{orb} ,^{18,19} one can presuppose that it should also lead to a better ratio of the L_3 and L_2 XMCD peak intensities because these are, within certain considerations, related to μ_{orb} .⁶

This paper reports on an application of the LSDA+DMFT formalism to x-ray absorption spectroscopy focusing on the $L_{2,3}$ edge spectra of Fe, Co, and Ni. We demonstrate that accounting for the valence-band and conduction-band correlations via the LSDA+DMFT improves the calculated spectra with respect to the LSDA. However, the improvement still does not lead to a fully satisfying reproduction of the experimental data — not even if the core hole is included via the final state approximation. Based on these results, we conclude that dealing with the dynamical aspects of the correlations between the core hole and the valence and conduction electrons is needed for further investigations.

II. COMPUTATIONAL SCHEME

A detailed description of the implementation of the LSDA+DMFT within the Korringa-Kohn-Rostoker (KKR) band structure scheme can be found in previous publications.^{20,21} Accordingly, we summarize here just the major features. The LSDA+DMFT method belongs to Hubbard- U band-structure schemes, i.e., the one-electron LSDA Hamiltonian is extended by an additional Hubbard-Hamiltonian term which explicitly describes the on-site interaction between (in our case) the d electrons. The many-body Hamiltonian is specified by parameters representing the Coulomb matrix elements.

The main idea of the DMFT is to map the periodic many-body problem onto an effective single-impurity problem that has to be solved self-consistently. For this purpose one describes the electronic properties of the system in terms of the single particle Green's function $\hat{G}(E)$, which is determined by

$$\left[E - \hat{H}_{\text{LSDA}} - \hat{\Sigma}(E) \right] \hat{G} = \hat{1} \quad , \quad (1)$$

where E is the complex energy, \hat{H}_{LSDA} is the LSDA Hamiltonian and $\hat{\Sigma}$ is a single-site effective self-energy operator. Within the DMFT, the self-energy $\hat{\Sigma}(E)$ is a solution of the many-body problem of an impurity placed

in an effective medium. This medium is described by the so called *bath* Green's function \hat{G} connected to the Green's function $\hat{G}(E)$ by

$$\hat{G}^{-1}(E) = \hat{G}^{-1}(E) + \hat{\Sigma}(E) \quad . \quad (2)$$

For a more detailed description of the DMFT equations the authors redirect the reader to one of the excellent reviews.^{22,23}

The self-energy $\hat{\Sigma}(E)$ and the bath Green's function $\hat{G}(E)$ have to be determined self-consistently. Technically, this is done in two steps. The first step is solving Eq. (1) by the means of spin-polarized fully relativistic KKR band structure method.²⁴ We relied on the atomic sphere approximation (ASA) to the potential and used an angular momentum cut-off $\ell_{\text{max}}=3$. The integration over the \mathbf{k} points was done on a regular mesh, using 2600 points in the irreducible part of the Brillouin zone in the case of bcc Fe and fcc Ni and 900 points in the case of hcp Co. The Vosko, Wilk, and Nusair parametrization for the local exchange and correlation potential was used.²⁵

In the second step of the LSDA+DMFT calculation, the self-energy $\hat{\Sigma}(E)$ has to be found according to Eq. (2). This is done by solving the many-body effective impurity problem, often referred to as the DMFT solver.^{22,23} We used perturbative solvers, either the spin-polarized T -matrix + FLEX solver²⁶ or the spin-polarized T -matrix approximation solver (TMA).²⁷ The use of perturbative solvers is justified because the correlation effects in pure $3d$ TMs are not very pronounced. The results are very similar for both solvers. Unless explicitly stated otherwise, data for the TMA solver are shown here. For the intra-atomic Hund exchange interaction J we take a common value of $J=0.9$ eV.^{23,28} The screened on-site Coulomb interaction U is set to 1.7 eV for Fe, 2.3 eV for Co, and 2.8 eV for Ni. These values were chosen because they lead to good values of μ_{spin} and μ_{orb} (see Chadov *et al.*¹⁸ for an extensive study) and also to a correct description of angular resolved photoemission spectra.^{15–17} Similar values of U and J were used also by other authors dealing with these systems,^{29–31} even though it should be noted that the parameters U and J are not directly transferable from one work to another because they depend, among others, on the choice of the basis set.²³

Our implementation of the LSDA+DMFT method is self-consistent not only in the self-energy $\hat{\Sigma}(E)$ but also in the charge density $\rho(\mathbf{r})$, i.e., in each iteration a new potential is used to generate a new single particle Green's function $\hat{G}(E)$ entering Eq. (2). During the self-consistency cycle, the self-energy $\hat{\Sigma}(E)$ is calculated either on a set of Matsubara frequencies (FLEX solver) or on the real energy axis (TMA solver). When calculating x-ray absorption spectra, the self-energy on the real axis above E_F is obtained via the Padé analytic continuation.³²

The LSDA accounts already to some extent for the correlation of the d electrons, so a corresponding term has to be subtracted, to avoid counting this interaction

twice. The exact form of this “double counting term” is not available because the LSDA is not formulated in a diagrammatic language; the choice has to be made by an educated guess. One way of doing this is to make *a priori* assumptions about the occupation of the correlated orbitals. In the limit of a uniform occupancy of these orbitals, the energy correction to the LSDA is due to “fluctuations” away from the spin-dependent orbitally averaged occupation. The interaction term in this around mean-field (AMF) limit is³³

$$V_{m\sigma}^{\text{LSDA+AMF}} = \sum_{m'} U_{mm'} (n_{m'-\sigma} - n_{-\sigma}^0) \quad (3) \\ + \sum_{m' \neq m} (U_{mm'} - J_{mm'}) (n_{m'\sigma} - n_{\sigma}^0) .$$

In the above equation, $n_{m\sigma}$ is the occupation number for electrons with orbital and spin quantum numbers m and σ , n_{σ}^0 is the orbitally averaged occupation number and $U_{mm'}$ and $J_{mm'}$ are matrix elements defined by the parameters U and J . The opposite limiting case concerning the occupation of the orbitals is the around atomic limit (AAL), which produces the correct behavior if $n_{m\sigma}=0$ or 1. It is sometimes referred to as the fully localized limit (FLL) and the corresponding interaction term is³³

$$V_{m\sigma}^{\text{LSDA+AAL}} = V_{m\sigma}^{\text{LSDA+AMF}} - (U - J)(n_{\sigma}^0 - \frac{1}{2}) . \quad (4)$$

The results of the LSDA+ U or LSDA+DMFT calculations may strongly depend on the choice of the double counting (d.c.) procedure. Based on earlier works, especially in the field of photoemission, it appears that the AMF recipe is the most appropriate for the 3d TMs.^{16,17} It is interesting to see whether this recipe works also for x-ray absorption spectroscopy (XAS).

We investigate also the effect of the core hole treated within the final state approximation as fully relaxed and screened, i.e., with the potential calculated with one electron transferred from the 2p core level into the valence band. This was achieved by first performing a self-consistent calculation without the core hole and then by treating the photoabsorbing atom with the core hole as a perturbation, employing the impurity cluster Green’s function method.^{34–36} In this impurity calculation the electronic structure was allowed to relax within the first two nearest-neighbor atomic shells around the photoabsorbing atom.

The theoretical spectra were broadened to account for the finite lifetimes of the core hole and of the photoelectron. The core hole related broadening was simulated by a Lorentzian with full width at half maxima of 0.40 eV at the L_3 edge and 0.70 eV at the L_2 edge, which is in the range of generally accepted values.^{37,38} The excited photoelectron related broadening was simulated by a Lorentzian with energy-dependent width, according to the “universal curve” as suggested by Müller *et al.*³⁹ By optimizing the broadening along the suggestion of Benfatto *et al.*⁴⁰ a better visual agreement of our calculations

with experiment could be achieved. However, this would have no influence on the conclusions.

Intuitive understanding as well as quantitative analysis of XMCD spectra has been greatly helped by the XMCD sum rules. These rules associate areas of XANES and XMCD peaks with μ_{spin} and μ_{orb} of the photoabsorbing atom. Our calculations provide μ_{spin} and μ_{orb} as well as XANES and XMCD spectra. Accordingly, application of the sum rules to our calculated spectra makes it possible to assess to what extent the changes in the spectra caused by including the valence- and conduction-band correlations via the LSDA+DMFT are consistent with the corresponding changes in the magnetic moments.

For the $L_{2,3}$ edge spectra the sum rules can be written as^{6,7,41}

$$\frac{3}{I} \int (\Delta\mu_{L_3} - 2\Delta\mu_{L_2}) dE = \frac{\mu_{\text{spin}}^{(d)} + 7T_z^{(d)}}{n_h^{(d)}} \quad (5)$$

and

$$\frac{2}{I} \int (\Delta\mu_{L_3} + \Delta\mu_{L_2}) dE = \frac{\mu_{\text{orb}}^{(d)}}{n_h^{(d)}} , \quad (6)$$

where $\Delta\mu_{L_{2,3}}$ are the differences $\Delta\mu = \mu^{(+)} - \mu^{(-)}$ between the absorption coefficients for the left and right circularly polarized light at the L_2 and L_3 edges, I is the integrated isotropic absorption spectrum, $\mu_{\text{spin}}^{(d)}$ and $\mu_{\text{orb}}^{(d)}$ are the d components of the local spin and orbital magnetic moments, $n_h^{(d)}$ is the number of holes in the d band and $T_z^{(d)}$ is the d component of the intra-atomic magnetic dipole operator for spin quantization axis aligned along z . The $T_z^{(d)}$ term is negligible for high-symmetry systems as those dealt with here. However, this does not necessarily apply to more complex systems.⁴² Application of the sum rules (5)–(6) requires setting the energy cut-off E_C which defines the upper boundary of the 3d band. We determined it by requiring that the integrated density of the d states is 10 when integrated from the bottom of the valence band up to E_C , similar as in our earlier study.⁴²

III. EXPERIMENT

The bulk-like Fe, Co, and Ni films were grown *in situ* directly at the synchrotron radiation facility BESSY II (Berlin, Germany). As the substrate a Cu(100) single crystal was used and the films were prepared at room temperature in ultra high vacuum conditions (base pressure 2×10^{-10} mbar) by evaporation from high purity rods using a commercial triple e⁻-beam evaporator. The surface of the Cu crystal was cleaned by several cycles of Ar⁺ bombardment and annealing at $T=900$ K. The deposition rates were in the regime of 1 Å per minute. The Cu(100) single crystal and the films were characterized by means of low energy electron diffraction (LEED) and Auger-electron spectroscopy (AES). The thickness of the

TABLE I. Magnetic moments (in units of μ_B) for Fe, Co, and Ni calculated via the plain LSDA and via the LSDA+DMFT with the AMF d.c. correction.

	Fe	Co	Ni
μ_{spin} (LSDA)	2.26	1.60	0.63
μ_{spin} (LSDA+DMFT)	2.18	1.65	0.68
μ_{orb} (LSDA)	0.052	0.079	0.051
μ_{orb} (LSDA+DMFT)	0.094	0.155	0.071

ferromagnetic films was calibrated by AES and by the signal-to-background ratio (edge jump) at the respective $L_{2,3}$ -edges. The thickness of the Fe film was 50 monolayers (ML), and was 20 ML for the Co and Ni films. The experimental data have been obtained accounting for saturation effects, and the XMCD spectra have been corrected to correspond to 100 % circular polarization and collinear orientation of the photon \mathbf{k} -vector and the magnetization. Details on the sample preparation can be found in earlier works.^{43,44}

IV. RESULTS AND DISCUSSION

A. Magnetic moments

Generally, if correlations are included via the DMFT, the spin magnetic moment μ_{spin} of $3d$ TMs changes only slightly while the orbital magnetic moment μ_{orb} significantly increases.¹⁸ This is also illustrated by our results summarized in Tab. I. We show results for the FLEX solver, the results for the TMA solver differ by 3% at most. A detailed investigation of the influence of the model parameters on magnetic moments has been done by Chadov *et al.*¹⁸

B. Shape of spectral peaks

$L_{2,3}$ edge XANES and XMCD spectra calculated using the plain LSDA and using the LSDA+DMFT with the AMF d.c. correction are shown in Fig. 1, together with experimental data. One can see that including the correlations in the d band changes the peak intensities as well as the shapes of the main peaks. In particular, a more pronounced asymmetry of the L_3 peak appears in the LSDA+DMFT spectra, leading to a better agreement with experiment. The changes are, nevertheless, not very big. This may appear surprising given the fact that for photoemission spectra of these systems, the inclusion of dynamic correlations via the LSDA+DMFT has a very pronounced effect as compared to the LSDA.¹⁵ However, the self-energy $\hat{\Sigma}(E)$ is relatively small in the regime of unoccupied states³⁰ so it is actually plausible that its effect on the XAS is not very pronounced.

As it was mentioned in the introduction, in order to remedy many deficiencies of the LSDA as concerns the

ground-state properties such as μ_{orb} it is sufficient to include the correlations in a static way only, via the OP Brooks scheme or via the LSDA+ U . However, these schemes do not bring any significant improvement concerning XAS. We demonstrate this by showing in Fig. 2 spectra calculated via the LSDA and via the LSDA+ U (the dashed and dash-dotted lines). Spectra obtained via the OP Brooks scheme are practically indistinguishable from the LSDA+ U results, so they are not shown here. Fig. 2 shows that the LSDA+ U method does not significantly alter the calculated spectra of transition metals with respect to the LSDA, similarly as it was found earlier for the OP Brooks scheme.⁴⁵ This is in line with the concept that the OP Brooks scheme can be seen in fact as one of the limits of the more general LSDA+ U concept.¹³

It was mentioned earlier in Sec. II that there are several ways to correct for the d.c. error in the LSDA+DMFT. Even though the AMF scheme seems to be the most reasonable d.c. procedure for $3d$ TMs, one cannot *a priori* exclude the possibility that another d.c. scheme might be more appropriate for XAS. Therefore, we checked how the results change if the AAL d.c. scheme is employed instead of the AMF scheme. We found that the calculated spectra look quite similar (Fig. 2, dotted lines and full lines). A closer inspection of Fig. 2 reveals further that the calculated spectra split into two groups, according to whether the *dynamic effects* to the self-energy have been included (LSDA+DMFT calculations) or not (LSDA and LSDA+ U calculations). This is especially evident for the XANES spectra; e.g., in the case of Co, only two spectral curves can in fact be distinguished because the results are pairwise practically identical (upper part of the middle panel in Fig. 2). For the XMCD spectra, this splitting of the four spectra into two groups is clearly visible at the high-energy end of the Fe and Co L_3 peaks, between 1–3 eV in Fig. 2. The choice of the d.c. model has thus only a minor influence on the shapes of XANES and XMCD spectra. Nevertheless, it has some influence on the intensities of the peaks (see the following section).

C. Relation to the $\mu_{\text{orb}}^{(d)}/\mu_{\text{spin}}^{(d)}$ ratio

The changes in the XANES and XMCD spectra which result from the inclusion the d band correlations are not very pronounced. One may ask to what degree are the changes significant at all: do they really reflect the different treatment of the correlations? The significance of the changes in the spectra can be assessed by comparing them with the changes of the ground-state properties. A suitable quantity in this respect is the $\mu_{\text{orb}}/\mu_{\text{spin}}$ ratio, as it is underestimated by the plain LSDA while it is correctly described by the LSDA+DMFT method. By applying the XMCD sum rules (5)–(6) to the theoretical spectrum, the ratio between the d components of the magnetic moments, $\mu_{\text{orb}}^{(d)}/\mu_{\text{spin}}^{(d)}$, can be obtained and compared to the $\mu_{\text{orb}}^{(d)}/\mu_{\text{spin}}^{(d)}$ ratio obtained directly from

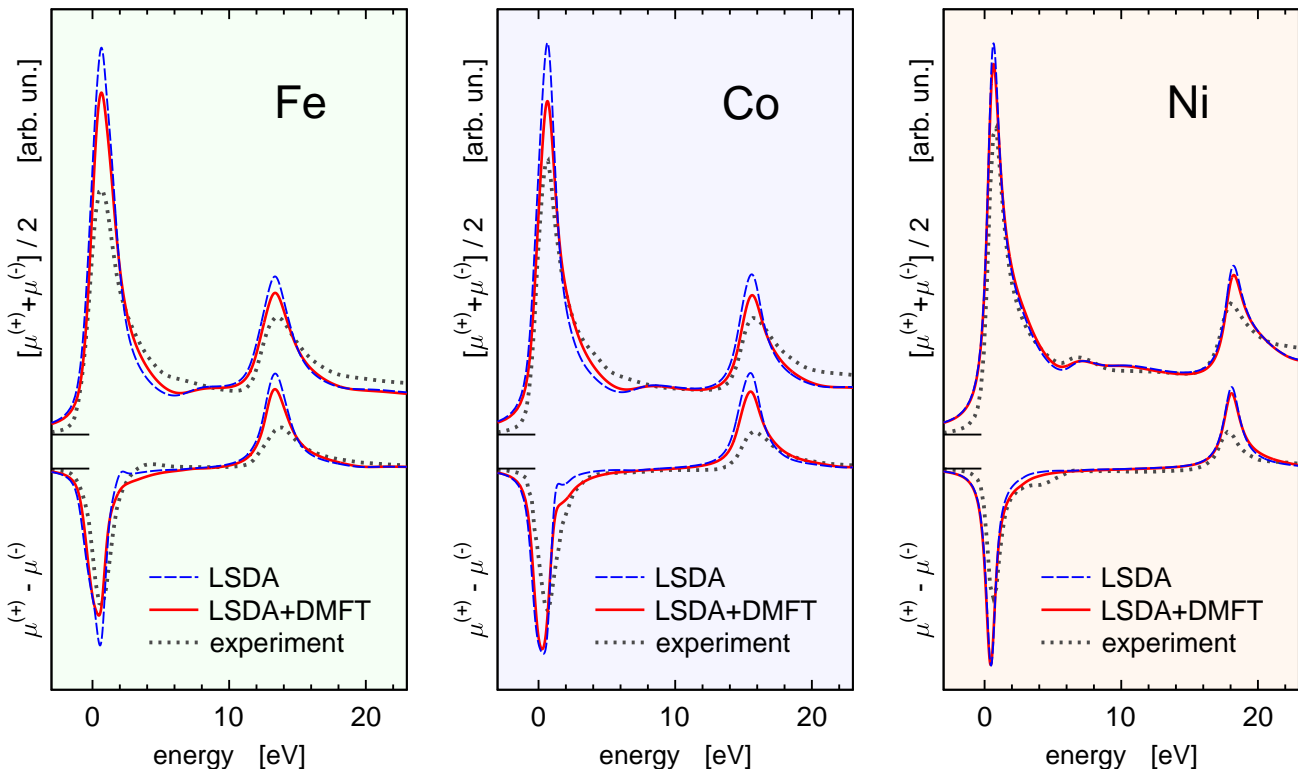


FIG. 1. (Color online) $L_{2,3}$ edge XANES and XMCD spectra of Fe, Co, and Ni calculated on the basis of the plain LSDA and of the LSDA+DMFT with the AMF d.c. correction, compared to experiment.

the ground-state electronic structure. If this is done for different ways of accounting for the many body effects, the consistency of the changes in the spectra and in the ground-state properties can be monitored.

Our results are summarized in Fig. 3, where the $\mu_{\text{orb}}^{(d)}/\mu_{\text{spin}}^{(d)}$ ratio evaluated by the two ways mentioned above is shown for the plain LSDA, the OP Brooks scheme, the LSDA+ U and the LSDA+DMFT with the AMF d.c. correction and the LSDA+ U and the LSDA+DMFT with the AAL d.c. correction. The $\mu_{\text{orb}}/\mu_{\text{spin}}$ ratio derived from magneto-mechanical experiments is shown for comparison.⁴⁶ Use of $\mu_{\text{orb}}/\mu_{\text{spin}}$ instead of $\mu_{\text{orb}}^{(d)}/\mu_{\text{spin}}^{(d)}$ as an experimental reference is justified because both ratios differ by less than 5% and our focus is not on the agreement of μ_{orb} with experiment (μ_{orb} depends also on the value of U anyway).¹⁸

It is obvious that the changes of the intensities of the L_3 and L_2 XMCD peaks reflect changes in $\mu_{\text{orb}}/\mu_{\text{spin}}$ via the sum rules very accurately. The differences between spectra calculated by different ways of dealing with the many body effects are thus relevant and consistent. Even relatively small changes in the intensities of XMCD peaks in Fig. 1 correspond to large changes in μ_{orb} , as can be seen in Tab. I. The failure of the LSDA to reproduce the ratio of the L_3/L_2 XMCD peak intensities thus cannot be a simple consequence of the failure of the LSDA to yield correct orbital moments μ_{orb} .

D. Effect of the core hole within the final state approximation

Accounting for the correlations in the d band via the LSDA+DMFT improves the calculated spectra but the improvement is not dramatic (Fig. 1). A better agreement with experiment could presumably be obtained if the core hole was accounted for. This is quite a complicated task within the *ab initio* scheme. A technically relatively simple way of achieving this is via the “static” final state approximation (see Sec. II). For the K edges, such a scheme sometimes improves the XANES (e.g., for the Zn edge in ZnSe⁴⁷ or for the Si edge in quartz)⁴⁸ while sometimes it has only a minor effect (early transition metals).³⁵ However, the final state approximation need not work for the $L_{2,3}$ edges which involve transitions to semi-localized d states: by promoting a $2p$ electron into the valence states one may effectively fill the d band of the photoabsorbing atom, suppressing to a large extent the intensity of the white line. This issue will be explored in the following.

To see the effect of the final state approximation, we applied it on top of the LSDA+DMFT procedure. The results are shown in Fig. 4. It is evident that this procedure does not generally improve the $L_{2,3}$ edge spectra of late $3d$ TMs. Hardly any systematic trend in the effect of the core hole can be found — neither as concerns

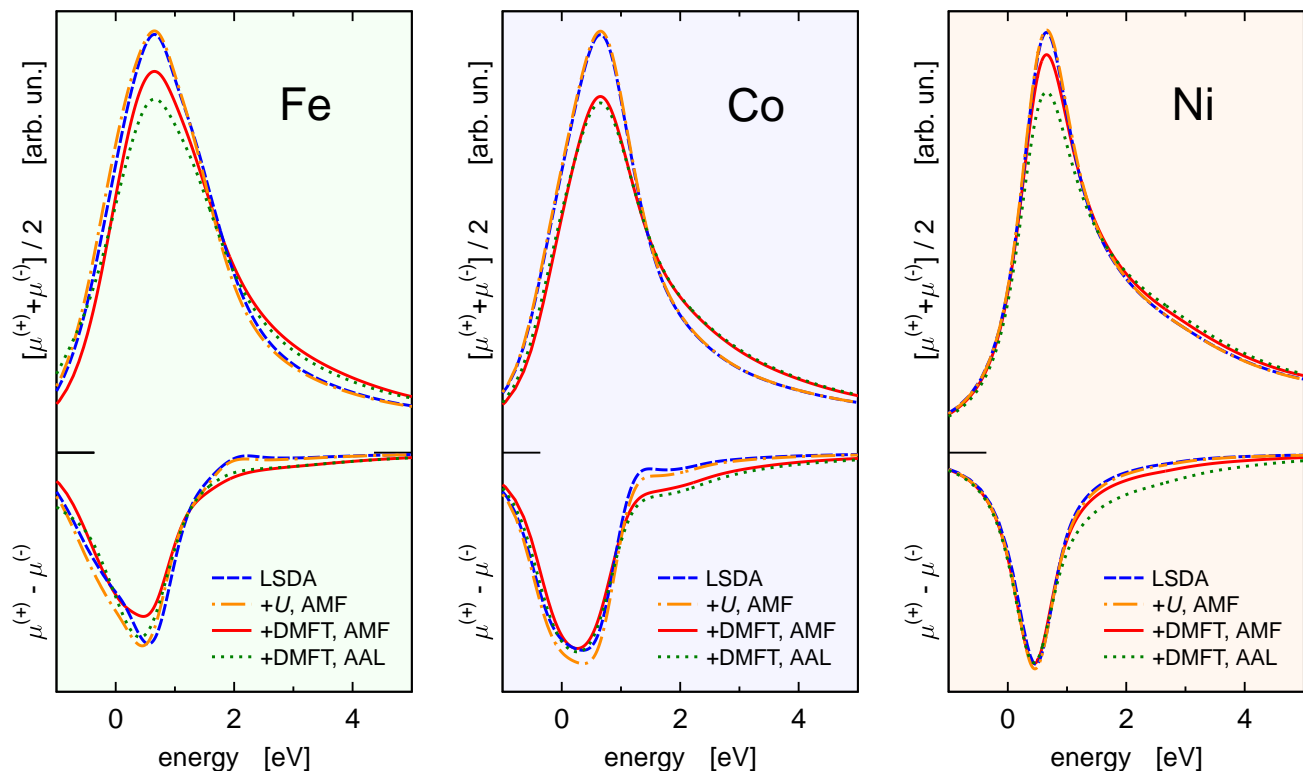


FIG. 2. (Color online) L_3 edge XANES and XMCD spectra for Fe, Co, and Ni calculated on the basis of the plain LSDA, via the LSDA+ U with the AMF d.c. correction, via the LSDA+DMFT with the AMF d.c. correction and via the LSDA+DMFT with the AAL d.c. correction.

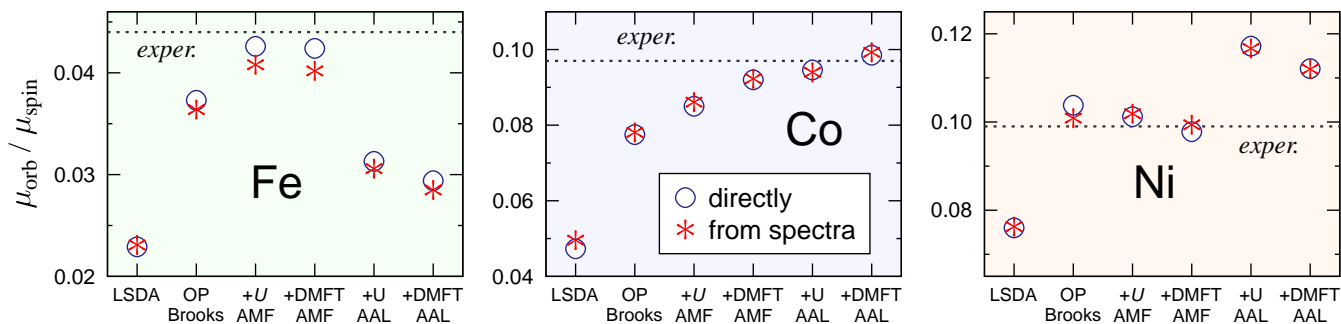


FIG. 3. (Color online) The $\mu_{\text{orb}}^{(d)} / \mu_{\text{spin}}^{(d)}$ ratio evaluated directly and from theoretical XMCD spectra for calculations employing plain LSDA, OP Brooks, LSDA+ U with the AMF d.c. correction (denoted as “+ U AMF” on the horizontal axis), LSDA+DMFT with the AMF d.c. correction (“+DMFT AMF”), LSDA+ U with the AAL d.c. correction (“+ U AAL”) and LSDA+DMFT with the AAL d.c. correction (“+DMFT AAL”). The experimental ratios were taken those obtained from magneto-mechanical measurements.⁴⁶

the shape of the white lines, nor as concerns the ratio of the intensities of the L_3 and L_2 peaks. For Fe, we observe an increase of the ratio of intensities of the L_3 and L_2 XMCD peaks, in agreement with experiment. For Co, the final state approximation produces only minor changes with respect to the ground state calculations. For Ni, however, including the core hole via the final state approximation substantially worsens the agreement with experiment — the XAS white lines as well as the

prominent XMCD peaks practically disappear! A similar situation occurs if the final state approximation is applied over the plain LSDA (therefore, only the LSDA+DMFT results are shown here).

We tested this scheme also by using a half-filled core hole, i.e., employing the Slater transition state method. Sometimes this procedure works well for the K edge spectra.^{49,50} Satisfying results were also reported for the Cu L_3 edge XANES.⁵¹ In our case, however, the Slater

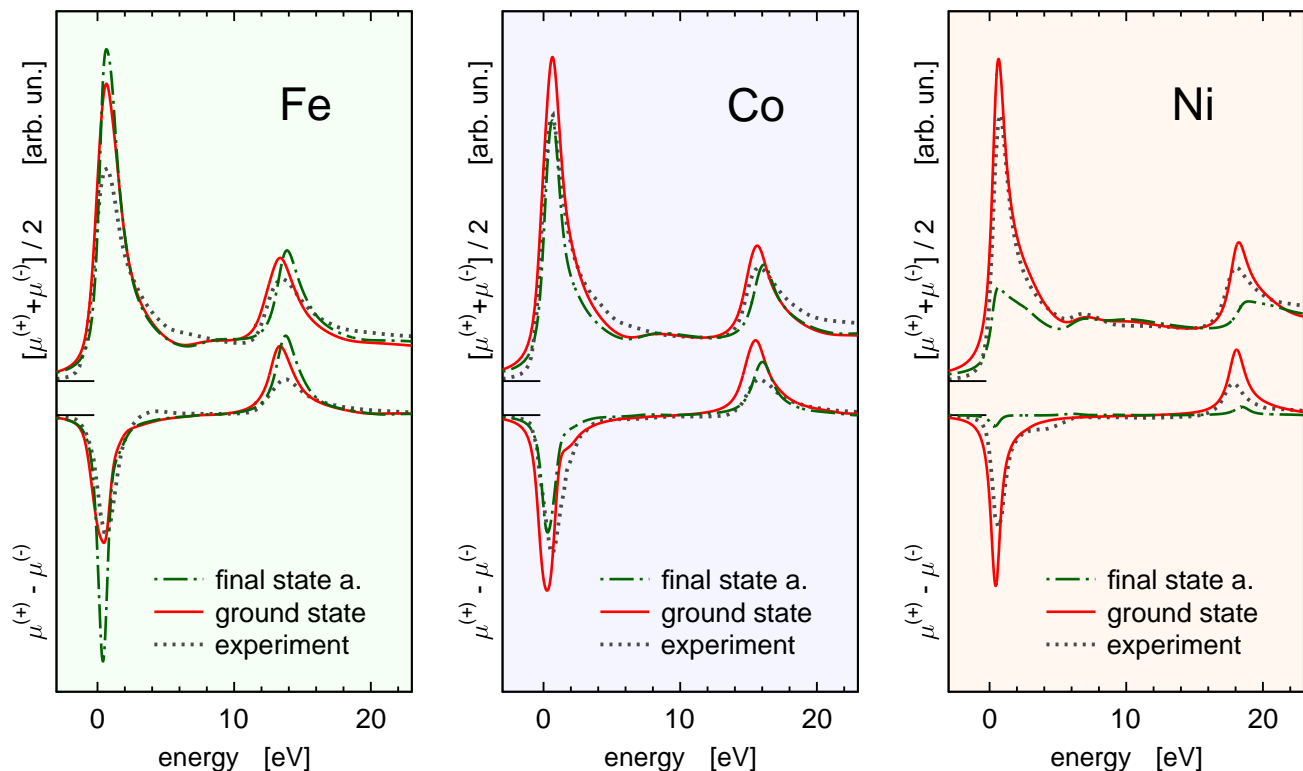


FIG. 4. (Color online) $L_{2,3}$ edge XANES and XMCD spectra of Fe, Co, and Ni calculated within the LSDA+DMFT when the core hole is ignored (using the ground state potential) and when the core hole is included via the final state approximation. Experimental XANES and XMCD spectra are shown for comparison.

transition state method does not bring any substantial improvement — the results just lie approximately halfway between the results obtained without a core hole and with a full core hole, so they are not shown here.

Our results demonstrate that the final state approximation is unsuitable for describing the $L_{2,3}$ edge XAS in late $3d$ TMs. This applies for calculations based on the plain LSDA as well as on the LSDA+DMFT method.

V. CONCLUSIONS

Our goal was to find out whether the differences commonly occurring between the experimental $L_{2,3}$ edge XANES and XMCD spectra of $3d$ transition metals on the one hand and *ab-initio* calculations on the other hand are mainly due to the way the LSDA deals with the correlations. By performing the LSDA+DMFT calculations, we found that if valence- and conduction-band correlations are included, the spectra change in the right direction with respect to the plain LSDA. In particular, the LSDA+DMFT yields asymmetric L_3 XAS white lines. The improvement is, however, rather incremental than dramatic. The ratio of the intensities of the L_3 and L_2

XAS and XMCD peaks is not significantly improved by the LSDA+DMFT formalism. The changes in the intensities of the XMCD peaks are, nevertheless, consistent with the changes of the $\mu_{\text{orb}}/\mu_{\text{spin}}$ ratio as suggested by the XMCD sum rules.

When the core hole is additionally accounted for within the final state approximation, the agreement between theory and experiment generally does not improve (in the case of Ni, it substantially worsens). It appears, therefore, that to get a decisive improvement of *ab-initio* calculations of the $L_{2,3}$ edge XAS and XMCD spectra of $3d$ metals, the dynamic correlations between the excited photoelectron and the core hole have to be taken into account.

ACKNOWLEDGMENTS

This work was supported by the Grant Agency of the Czech Republic within the project 108/11/0853, by the Deutsche Forschungsgemeinschaft through FOR 1346 and by the German ministry BMBF under contract 05KS10WMA. The research in the Institute of Physics AS CR was supported by the Academy of Sciences of the Czech Republic.

- * sivr@fzu.cz; <http://www.fzu.cz/~sivr>
- † Hubert.Ebert@cup.uni-muenchen.de;
<http://ebert.cup.uni-muenchen.de>
- ¹ H. Wende, Rep. Prog. Phys. **67**, 2105 (2004).
 - ² J. Schwitalla and H. Ebert, Phys. Rev. Lett. **80**, 4586 (1998).
 - ³ A. L. Ankudinov, A. I. Nesvizhskii, and J. J. Rehr, Phys. Rev. B **67**, 115120 (2003).
 - ⁴ M. Alouani, J. M. Wills, and J. W. Wilkins, Phys. Rev. B **57**, 9502 (1998).
 - ⁵ O. Šipr and H. Ebert, Phys. Rev. B **72**, 134406 (2005).
 - ⁶ P. Carra, B. T. Thole, M. Altarelli, and X. Wang, Phys. Rev. Lett. **70**, 694 (1993).
 - ⁷ B. T. Thole, P. Carra, F. Sette, and G. van der Laan, Phys. Rev. Lett. **68**, 1943 (1992).
 - ⁸ A. Scherz, H. Wende, K. Baberschke, J. Minár, D. Benea, and H. Ebert, Phys. Rev. B **66**, 184401 (2002).
 - ⁹ K. Baberschke, Physica Scripta **T115**, 49 (2005).
 - ¹⁰ H. Wende, A. Scherz, C. Sorg, K. Baberschke, E. K. U. Gross, H. Appel, K. Burke, J. Minár, H. Ebert, A. L. Ankudinov, and J. J. Rehr, AIP Conference Proceedings **882**, 78 (2007).
 - ¹¹ O. Eriksson, B. Johansson, R. C. Albers, A. M. Boring, and M. S. S. Brooks, Phys. Rev. B **42**, 2707 (1990).
 - ¹² I. V. Solovyev, Phys. Rev. Lett. **95**, 267205 (2005).
 - ¹³ I. V. Solovyev, A. I. Liechtenstein, and K. Terakura, Phys. Rev. Lett. **80**, 5758 (1998).
 - ¹⁴ J. Minár, H. Ebert, C. De Nadaï, N. B. Brookes, F. Venturini, G. Ghiringhelli, L. Chioncel, M. I. Katsnelson, and A. I. Lichtenstein, Phys. Rev. Lett. **95**, 166401 (2005).
 - ¹⁵ J. Braun, J. Minár, H. Ebert, M. I. Katsnelson, and A. I. Lichtenstein, Phys. Rev. Lett. **97**, 227601 (2006).
 - ¹⁶ J. Sánchez-Barriga, J. Fink, V. Boni, I. Di Marco, J. Braun, J. Minár, A. Varykhalov, O. Rader, V. Bellini, F. Manghi, H. Ebert, M. I. Katsnelson, A. I. Lichtenstein, O. Eriksson, W. Eberhardt, and H. A. Dürr, Phys. Rev. Lett. **103**, 267203 (2009).
 - ¹⁷ J. Sánchez-Barriga, J. Minár, J. Braun, A. Varykhalov, V. Boni, I. Di Marco, O. Rader, V. Bellini, F. Manghi, H. Ebert, M. I. Katsnelson, A. I. Lichtenstein, O. Eriksson, W. Eberhardt, H. A. Dürr, and J. Fink, Phys. Rev. B **82**, 104414 (2010).
 - ¹⁸ S. Chadov, J. Minár, M. I. Katsnelson, H. Ebert, D. Ködderitzsch, and A. I. Lichtenstein, Europhys. Lett. **82**, 37001 (2008).
 - ¹⁹ O. Šipr, J. Minár, S. Mankovsky, and H. Ebert, Phys. Rev. B **78**, 144403 (2008).
 - ²⁰ J. Minár, L. Chioncel, A. Perlov, H. Ebert, M. I. Katsnelson, and A. I. Lichtenstein, Phys. Rev. B **72**, 045125 (2005).
 - ²¹ J. Minár, Psi-k Newsletter Highlight 101 (2010).
 - ²² G. Kotliar, S. Y. Savrasov, K. Haule, V. S. Oudovenko, O. Parcollet, and C. A. Marianetti, Rev. Mod. Phys. **78**, 865 (2006).
 - ²³ K. Held, Adv. Phys. **56**, 829 (2007).
 - ²⁴ H. Ebert, in *Electronic Structure and Physical Properties of Solids*, Lecture Notes in Physics, Vol. 535, edited by H. Dreyssé (Springer, Berlin, 2000) p. 191.
 - ²⁵ S. H. Vosko, L. Wilk, and M. Nusair, Can. J. Phys. **58**, 1200 (1980).
 - ²⁶ L. V. Pourovskii, M. I. Katsnelson, and A. I. Lichtenstein, Phys. Rev. B **72**, 115106 (2005).
 - ²⁷ S. Chadov, Ph.D. thesis, Universität München (2007).
 - ²⁸ V. I. Anisimov and O. Gunnarsson, Phys. Rev. B **43**, 7570 (1991).
 - ²⁹ I. Yang, S. Y. Savrasov, and G. Kotliar, Phys. Rev. Lett. **87**, 216405 (2001).
 - ³⁰ A. Grechnev, I. Di Marco, M. I. Katsnelson, A. I. Lichtenstein, J. Wills, and O. Eriksson, Phys. Rev. B **76**, 035107 (2007).
 - ³¹ O. Miura and T. Fujiwara, Phys. Rev. B **77**, 195124 (2008).
 - ³² H. J. Vidberg and J. W. Serene, J. Low Temp. Phys. **29**, 179 (1977).
 - ³³ M. T. Czyzyk and G. A. Sawatzky, Phys. Rev. B **49**, 14211 (1994).
 - ³⁴ P. J. Braspenning, R. Zeller, A. Lodder, and P. H. Dederichs, Phys. Rev. B **29**, 703 (1984).
 - ³⁵ R. Zeller, Z. Physik B **72**, 79 (1988).
 - ³⁶ K. Jorissen and J. J. Rehr, Phys. Rev. B **81**, 245124 (2010).
 - ³⁷ F. A. Shamma, M. Abbate, and J. C. Fuggle, in *Unoccupied Electron States*, edited by J. C. Fuggle and J. E. Inglesfield (Springer Verlag, Berlin, 1992) p. 347.
 - ³⁸ J. L. Campbell and T. Papp, At. Data Nucl. Data Tables **7**, 1 (2001).
 - ³⁹ J. E. Müller, O. Jepsen, and J. W. Wilkins, Solid State Commun. **42**, 365 (1982).
 - ⁴⁰ M. Benfatto, S. Della Longa, and C. R. Natoli, J. Synchr. Rad. **10**, 51 (2003).
 - ⁴¹ J. Stöhr, J. Magn. Magn. Materials **200**, 470 (1999).
 - ⁴² O. Šipr, J. Minár, and H. Ebert, Europhys. Lett. **87**, 67007 (2009).
 - ⁴³ A. Scherz, H. Wende, and K. Baberschke, Appl. Physics A **78**, 843 (2004).
 - ⁴⁴ A. Scherz, Ph.D. thesis, Freie Universität Berlin (2004).
 - ⁴⁵ H. Ebert, Solid State Commun. **100**, 677 (1996).
 - ⁴⁶ R. A. Reck and D. L. Fry, Phys. Rev. **184**, 492 (1969).
 - ⁴⁷ O. Šipr, P. Machek, A. Šimůnek, J. Vackář, and J. Horák, Phys. Rev. B **56**, 13151 (1997).
 - ⁴⁸ Z. Y. Wu, F. Jollet, and F. Seifert, J. Phys.: Condens. Matter **10**, 8083 (1998).
 - ⁴⁹ T. Mizoguchi, I. Tanaka, M. Yoshiya, F. Oba, K. Ogasawara, and H. Adachi, Phys. Rev. B **61**, 2180 (2000).
 - ⁵⁰ M. Leetmaa, M. P. Ljungberg, A. Lyubartsev, A. Nilsson, and L. G. M. Pettersson, J. Electron. Spectrosc. Relat. Phenom. **177**, 135 (2010).
 - ⁵¹ J. Luitz, M. Maier, C. Hébert, P. Schattschneider, P. Blaha, K. Schwarz, and B. Jouffrey, Eur. Phys. J. B **21**, 363 (2001).